Published in final edited form as:
J Neurovirol. 2012 August ; 18(4): 303–312. doi:10.1007/s13365-012-0106-1.

Cerebrovascular risk factors and brain microstructural abnormalities on diffusion tensor images in HIV-infected individuals

Beau K. Nakamoto,
University of Hawaii, Honolulu, HI, USA

Straub Clinics and Hospital, Honolulu, HI, USA

Hawaii Center for AIDS, John A. Burns School of Medicine, University of Hawaii at Manoa, 3675 Kilauea Ave. Young Bldg 5th Floor, Honolulu, HI 96816, USA

Neda Jahanshad,
Laboratory of Neuro Imaging, Departments of Neurology and Psychiatry, UCLA School of Medicine, Los Angeles, CA, USA

Aaron McMurtray,
Ventura County Medical Center, Ventura, CA, USA

Kalpana J. Kallianpur,
University of Hawaii, Honolulu, HI, USA

Dominic C. Chow,
University of Hawaii, Honolulu, HI, USA

Victor G. Valcour,
University of California at San Francisco, San Francisco, CA, USA

Robert H. Paul,
University of Missouri, St. Louis, MO, USA

Liron Marotz,
University of Hawaii, Honolulu, HI, USA

Paul M. Thompson, and
Laboratory of Neuro Imaging, Departments of Neurology and Psychiatry, UCLA School of Medicine, Los Angeles, CA, USA

Cecilia M. Shikuma
University of Hawaii, Honolulu, HI, USA

Beau K. Nakamoto: beau_nakamoto@yahoo.com

Abstract

HIV-associated neurocognitive disorder remains prevalent in HIV-infected individuals despite effective antiretroviral therapy. As these individuals age, comorbid cerebrovascular disease will likely impact cognitive function. Effective tools to study this impact are needed. This study used diffusion tensor imaging (DTI) to characterize brain microstructural changes in HIV-infected

Correspondence to: Beau K. Nakamoto, beau_nakamoto@yahoo.com.

Beau K. Nakamoto and Neda Jahanshad contributed equally to this manuscript.

individuals with and without cerebrovascular risk factors. Diffusion-weighted MRIs were obtained in 22 HIV-infected subjects aged 50 years or older (mean age = 58 years, standard deviation = 6 years; 19 males, three females). Tensors were calculated to obtain fractional anisotropy (FA) and mean diffusivity (MD) maps. Statistical comparisons accounting for multiple comparisons were made between groups with and without cerebrovascular risk factors. Abnormal glucose metabolism (i.e., impaired fasting glucose, impaired glucose tolerance, or diabetes mellitus) was associated with significantly higher MD (false discovery rate (FDR) critical p value = 0.008) and lower FA FDR critical p value = 0.002) in the caudate and lower FA in the hippocampus (FDR critical p value = 0.004). Pearson correlations were performed between DTI measures in the caudate and hippocampus and age- and education-adjusted composite scores of global cognitive function, memory, and psychomotor speed. There were no detectable correlations between the neuroimaging measures and measures of cognition. In summary, we demonstrate that brain microstructural abnormalities are associated with abnormal glucose metabolism in the caudate and hippocampus of HIV-infected individuals. Deep gray matter structures and the hippocampus may be vulnerable in subjects with comorbid abnormal glucose metabolism, but our results should be confirmed in further studies.

Keywords

HIV; Cerebrovascular disease; Diffusion tensor imaging

Introduction

Cerebrovascular risk factors are prevalent in HIV-infected individuals. Several studies show that preexisting cerebrovascular risk factors (e.g., smoking, dyslipidemia, hypertension, and diabetes mellitus) are associated with cognitive impairment (Becker et al. 2009;Wright et al. 2010; Nakamoto et al. 2011).

Ovbiagele and Nath (2011) reported that the incidence of stroke hospitalizations with comorbid HIV infection rose 60 % between 1997 and 2006. In a study of 292 HIV-infected individuals with high CD4 cell counts (median CD4 cell count = 536 cells/mm^3) from the Strategies for Management of Antiretroviral Therapy study, patients with preexisting cardiovascular disease had a 6.2-fold higher odds of having cognitive impairment (Wright et al. 2010). Prior cardiovascular disease, hypertension, and hypercholesterolemia were also associated with worse cognitive performance as measured by a composite z score of information processing speed, attention, executive, and motor functions (Wright et al. 2010). Analysis of 428 HIV-infected older (≥40) gay and bisexual males from the Multicenter AIDS Cohort Study demonstrated that subclinical atherosclerosis as measured by carotid intima–media thickness was associated with worse psychomotor performance (Becker et al. 2009). The impact of cerebrovascular disease on cognitive function appears to be additive rather than synergistic with HIV infection (Nakamoto et al. 2010).

Infection with HIV is associated with atrophy in the cerebral cortex (e.g., anterior cingulate, insula, and superior frontal, orbitofrontal, parietal, posterior/inferior temporal lobes) (Becker et al. 2011a; Kuper et al. 2011; Kallianpur et al. 2011), deep gray matter (e.g., caudate, putamen) (Becker et al. 2011b), and lower white matter volume (Becker et al. 2011a). The additional impact of cerebrovascular risk factors on brain structure is unclear. One study by Becker et al. (2011a) did not detect an association between brain atrophy and cerebrovascular risk factors.

Diffusion tensor imaging (DTI) is a MRI technique which measures the random motion of water to assess the microstructural integrity of brain tissue. Mean diffusivity (MD) and

fractional anisotropy (FA) are two common DTI measures that describe the speed and direction of water diffusion within the brain. MD is a DTI measure of the diffusion speed of water molecules. In constricted regions (e.g., inside cells) where the diffusion of water molecules is slow, MD is low. In unconstricted regions (e.g., inside the ventricles), the diffusion of water molecules is relatively fast, and MD is high. FA is a DTI measure of the directionality of water diffusion. When the diffusion of water molecules is equal in all directions, diffusion is isotropic. The diffusion of water in gray matter is one example of isotropy. When the diffusion of water has directionality, the diffusion is anisotropic. The diffusion of water along axons in the white matter of the brain is one example of anisotropy where the diffusion of water is constrained by the axon's myelin sheath. Higher MD and lower FA values suggest decreased micro-structural integrity in the brain.

Several studies, some including HIV-infected populations, have used DTI to study the microstructure of white matter (Basser et al. 1994a, b; Filippi et al. 2001; Pfefferbaum et al. 2007, 2009; Gongvatana et al. 2009, 2011; Chen et al. 2009; Hoare et al. 2011) Little attention has been given to examine the deep gray matter or hippocampal microstructure in the HIV-infected population (Ragin et al. 2005; Chang et al. 2008). These regions of interest (ROIs) are relevant to HIV-infected individuals given the basal ganglia and hippocampus are preferential sites of neuropathology in HIV infection and cerebrovascular disease (Navia et al. 1986; Jellinger 2008; Gorelick and Bowler 2010). DTI can detect subtle microstructural brain changes event when there are no detectable macrostructural changes, such as atrophy, on standard MRI scans in HIV-infected individuals (Filippi et al. 2001). We hypothesized that cerebrovascular risk factors would be associated with DTI differences.

Methods

Study population

This study used data from a parent positron emission tomography (PET) study assessing the impact of the apolipoprotein epsilon 4 (APOE ε4) genotype on cortical metabolism in HIV-infected subjects at least 50 years of age. The PET results were presented elsewhere (McMurtray et al. 2008). Brain MRIs were obtained as an optional procedure in 22 subjects out of 27 subjects who were studied further here. These subjects are the focus of this analysis. The Committee on Human Studies at the University of Hawaii approved the protocol.

Clinical assessment

Demographic characteristics collected included age, sex, race/ethnicity, and self-reported years of education. General medical and current medication histories were collected. HIV-relevant characteristics collected included self-reported current and the lowest ever CD4+ lymphocyte cell count and current antiretroviral therapy. Measured biological characteristics included height, weight, waist circumference, blood pressure, plasma HIV RNA, CD4+ lymphocyte cell count, APOE ε4 genotype, fasting lipid profile, directly measured low-density lipoprotein (LDL) cholesterol, and fasting plasma glucose. We evaluated glucose homeostasis with a 2-h oral glucose tolerance test (OGTT).

Hypertension was defined as self-reported diagnosis, use of an antihypertensive medication, or measured systolic blood pressure (SBP) equal to or greater than 140 mmHg or diastolic blood pressure (DBP) equal to or greater than 90 mmHg (U.S. Preventive Services Task Force 2007). We defined diabetes mellitus as self-reported diagnosis, use of diabetes medication, or a fasting plasma glucose greater than 125 mg/dL or 2-h post-challenge glucose greater than or equal to 200 mg/dL (American Diabetes Association 2009). Impaired fasting glucose was defined as a fasting plasma glucose between 100 and 125 mg/dL and

impaired glucose tolerance as a 2-h post-challenge glucose between 140 and 199 mg/dL (American Diabetes Association 2009). We classified individuals as having abnormal glucose metabolism if they met criteria for impaired fasting glucose, impaired glucose tolerance, or diabetes mellitus. Elevated LDL cholesterol was defined as a fasting measured LDL cholesterol greater than or equal to 100 mg/dL (Expert Panel on Detection, Evaluation, and Treatment of High Blood Cholesterol in Adults 2002). Elevated triglyceride level was defined as a fasting triglyceride greater than or equal to 150 mg/dL (Expert Panel on Detection, Evaluation, and Treatment of High Blood Cholesterol in Adults 2001). Low high-density lipoprotein (HDL) cholesterol was defined as a fasting HDL cholesterol less than 40 mg/dL in men and less than 50 mg/dL in women (Expert Panel on Detection, Evaluation, and Treatment of High Blood Cholesterol in Adults 2001). Abdominal obesity was defined as a waist circumference in men greater than 102 cm (40 in.) and in women greater than 88 cm (35 in.) (Expert Panel on Detection, Evaluation, and Treatment of High Blood Cholesterol in Adults 2001). Waist circumference was recorded as a measure of abdominal obesity, as possible decreases in hip circumference due to lipodystrophy may make use of waist-to-hip ratio problematic (Brown et al. 2009). Diagnosis of the metabolic syndrome was based on Adult Treatment Panel III (ATP-III) criteria (Expert Panel on Detection, Evaluation, and Treatment of High Blood Cholesterol in Adults 2001). Depressive symptoms were assessed with the Beck Depression Inventory II (BDI-II) (Beck et al. 1961).

Diffusion tensor imaging

MRI scans were acquired within 1 month of clinical assessment and neuropsychological testing on the same Philips 3.0-T Achieva scanner equipped with an eight-channel sensitivity encoding head coil. For each subject, structural and diffusion-weighted MRI scans were obtained. Structural MRI included a sagittal T1-weighted image with a three-dimensional turbo field-echo sequence (repetition time/echo time (TR/TE)06.7/3.1 ms, flip angle 8°, slice thickness 1.2 mm, in-plane resolution 1.0 mm^2; Wright et al. 2010). Diffusion-weighted scans included a single-shot echo planar imaging sequence (24 cm field of view, TR/TE07,859 ms/80 ms, flip angle 90°, 3.0-mm-thick slices, 0 mm gap, SENSE factor = 3.1, maximum slew rate 120 mT/m/ms, gradient amplitude 40 mT/m, 96 × 95 acquisition matrix, 2.5 × 2.5 mm^2 inplane resolution, and a variable number of slices determined by head size). One image with no diffusion sensitization was obtained (i.e., a T2-weighted b_0 image). Diffusion weighting was applied along 15 non-collinear directions evenly distributed over a sphere with a *b*-factor of 1,000 s/mm^2 (Wright et al. 2010) and four signal averages to increase the signal-to-noise ratio. Scan time was 8.6 min.

The diffusion-weighted images were uploaded to the Laboratory of Neuro Imaging at the University of California, Los Angeles. Correction for subject motion inside the scanner and eddy current distortions were performed on the diffusion-weighted images using FSL software (http://fsl.fmrib.ox.ac.uk/fsl/). The correctly aligned images were then used to calculate the tensors from which MD and FA maps were created. Diffusion tensors were computed at each voxel using FSL software (http://fsl.fmrib.ox.ac.uk/fsl/). From the tensor eigenvalues (λ_1, λ_2, λ_3), FA was calculated according to the formula:

$$\mathrm{FA}=\sqrt{\frac{3}{2}}\frac{\sqrt{(\lambda_1-<\lambda>)^2+(\lambda_2-<\lambda>)^2+(\lambda_3-<\lambda>)^2}}{\sqrt{\lambda_1^2+\lambda_2^2+\lambda_3^2}}\in[0,1]<\lambda>=\frac{\lambda_1+\lambda_2+\lambda_3}{3}!$$

To assess the integrity of all images in the exact same locations, all images were registered to a template image. To preserve high anatomical resolution, a single subject with no anatomical abnormalities and with a high-quality scan was randomly selected as the target for the dataset. All subjects' b_0 images were aligned to the same space using linear

registration followed by an elastic inverse consistent mutual information-based nonlinear warping of all subject images to the target (Leow et al. 2005). For each subject, the transformation obtained from the linear registration and deformation field obtained from the nonlinear registration of subject to target b_0 images were then applied to the anisotropy and diffusivity images. Diffusion parameters (MD and FA) were measured voxelwise across the whole brain. Deep gray matter ROIs were manually extracted by the same neuroscientist (N.J.) from the target subject to include the caudate, putamen, globus pallidus, and thalamus. The corpus callosum which included the genu, body, and splenium in toto was also extracted. The mean FA and MD were then computed for each of the subjects, after their scans were registered to the selected target.

Neurocognitive testing

The neurocognitive battery tested seven cognitive domains: language (Boston Naming Test), verbal fluency (FAS letter fluency, animal naming), attention/working memory (WAIS-III Digit Span Subtest, WAIS-III Letter–Number Sequencing Subtest), speed of information processing (Trailmaking Test—Part A, California Computerized Assessment Package, WAIS-III Digit Symbol Subtest), executive function (Stroop Interference Test, Trailmaking Test—Part B), verbal and visual learning and memory (Rey Auditory Verbal Learning Test, Rey–Osterrieth Complex Figure Test), and motor skills (Grooved Pegboard Test, Timed Gait). Fasting laboratory measures and OGTT were performed on a different day from neurocognitive testing to minimize bias associated with fasting and the procedure (Lamport et al. 2009). Individual neuropsychological test scores were standardized based on age- and education-adjusted normative data to construct individual *z* scores (Strauss et al. 2006), and standardized unweighted composite *z* scores (age- and education-adjusted composite score of global cognitive function (NPZ-8), age- and education-adjusted composite score of memory (NPZ-3-mem), age- and education-adjusted composite score of psychomotor speed (NPZ-3-pm)) were derived by calculating the arithmetic mean of various individual *z* scores as previously described (Shiramizu et al. 2007). NPZ-8 is a measure of broader cognitive function by including eight tests thought to have specificity in HIV (Schmitt et al. 1988); NPZ-3-mem is a measure of memory; NPZ-3-pm is a measure of psychomotor speed. The composite *z* scores were defined so that positive values indicate better performance compared with age- and education-adjusted normative values, while negative values indicate poorer performance.

Statistical analysis

For DTI analysis, voxelwise statistical comparisons were made on diffusion parameters (MD and FA) between groups on spatially normalized and geometrically registered DTI-based diffusivity (MD) and anisotropy (FA) images in the whole brain. Additional ROIs were outlined on the template subjects and used as ROIs for which mean FA and MD values were compared across subjects. These ROIs include the corpus callosum, caudate, putamen, globus pallidus, and thalamus. Student's *t* tests were performed to compare the mean FA or MD values based on the presence or absence of each cerebrovascular risk factor (e.g., hypertension, abnormal glucose metabolism, metabolic syndrome, elevated total cholesterol, elevated LDL, past or present smoking history, and at least one APOE ε4 allele). Multiple comparison correction for the voxelwise tests was conducted using the false discovery rate (FDR) (Benjamini and Hochberg 1995). The cumulative distribution of *p* values was obtained in regions of high anisotropy (FA>0.3 for the group average) and plotted against the null distribution of *p* values where no significant differences (FDR controlling *p* value≤0.05) were detected on a voxelwise level. FDR was performed across the whole brain, corpus callosum, and four deep gray matter ROI for each cerebrovascular risk factor assessed. Pearson product–moment correlations were obtained between MD and FA values

in the statistically significant ROI and composite measures of neurocognitive performance (e.g., NPZ-8, NPZ-3-mem, NPZ-3-pm).

For clinical data, statistical analyses were performed with SAS 9.1 (Cary, NC, USA). Means, standard deviations, and proportions were calculated for baseline characteristics. The null hypothesis was that there was no association between neurocognitive composite scores and traditional cerebrovascular risk factors. NPZ-8, NPZ-3-mem, and NPZ-3-pm were used as dependent variables in three different linear regression models. Independent variables included age, current CD4+ count, self-reported lowest ever CD4+ count, SBP, DBP, LDL cholesterol, triglyceride, and HDL cholesterol as continuous variables and treatment with a protease inhibitor, abnormal glucose metabolism, and the presence of at least one APOE ε4 allele as categorical (present or absent) variables. Forward selection was used, and independent variables with p values less than or equal to 0.20 were included in the final regression model. A p value≤0.05 was considered statistically significant.

Results

Subject characteristics

The mean (standard deviation, SD) age of the sample was 58 (6) years (Table 1). All but one subject was on combination antiretroviral therapy (cART), and 20 of 21 were on the same cART regimen for 12 months. A minority (four of 22, 18 %) was treated with a protease inhibitor-based cART. All had current CD4+ counts >200 cells/μL. A majority (18 of 22, 82 %) had undetectable viral loads. The mean self-reported lowest ever CD4+ count was 210 cells/μL (SD 171 cells/μL). Subjects with a history of central nervous system opportunistic infection, seizures, head trauma with a loss of consciousness or cognitive sequelae, active psychosis, uncontrolled major affective disorders, and current substance abuse or dependence as defined by the *Diagnostic Statistical Manual of Mental Disorders* (American Psychiatric Association 2000) had been excluded from the parent study (McMurtray et al. 2008) from which these data were obtained.

Nine subjects had impaired fasting glucose or impaired glucose tolerance with one of these nine treated with metformin. Four subjects had diabetes mellitus among whom three were treated with either an oral antihyperglycemic or insulin, and the fourth subject was not on treatment. The rates of other cerebrovascular risk factors were high with seven meeting the definition of the metabolic syndrome as defined by ATP-III criteria (Expert Panel on Detection, Evaluation, and Treatment of High Blood Cholesterol in Adults 2001). Nine subjects had at least one APOE ε4 allele, and on average, these individuals were older (mean age = 62, SD = 7 versus 56, SD = 5 years; $p = 0.03$). However, there were no significant differences between the subjects with and without at least one APOE ε4 allele in mean SBP, DBP, fasting LDL, fasting triglycerides, fasting HDL, BMI, waist circumference, or proportion with abnormal glucose metabolism, or metabolic syndrome. The mean BDI-II score was 7 (SD, 4). No subjects had severe depression based on BDI-II.

Diffusion tensor imaging

Microstructural differences (i.e., higher MD, lower FA) were noted in the caudate and hippocampus of subjects with abnormal glucose metabolism in post hoc analysis (Table 2; Fig. 1). No hyperintensities were noted in the deep gray matter structures or hippocampus on visual inspection of T2-weighted sequences nor significant differences in the frequencies of individuals with a history of stimulant abuse between those with and without abnormal glucose metabolism ($p = 0.25$) to explain these results. We were unable to determine if there was an increased effect size in DTI measures between individuals with impaired fasting glucose/impaired glucose tolerance versus diabetes mellitus due to the small sample size. No

statistically significant correlations were found between MD and FA in the caudate and hippocampus and neurocognitive composite scores (i.e., NPZ-8, NPZ-3-mem, and NPZ-3-pm) by unadjusted Pearson correlation. There was a trend toward an inverse correlation between hippocampal MD and global cognitive function (NPZ-8; $r = -0.4381$, $p = 0.07$). No significant relationships were seen in MD and FA in the white matter (i.e., whole brain, corpus callosum), putamen, globus pallidus, or thalamus and other cerebrovascular risk factors (i.e., hypertension, metabolic syndrome, elevated total cholesterol, elevated LDL, past or present smoking history, and at least one APOE ε4 allele).

Neurocognitive testing

Age, abnormal glucose metabolism, metabolic syndrome, tobacco use, and the presence of at least one APOE ε4 allele met our criteria for inclusion using forward selection ($p \leq 0.20$) in the final multivariate analysis. Age ($\beta = -0.05$; $p = 0.02$), abnormal glucose metabolism ($\beta = 0.92$; $p < 0.01$), metabolic syndrome ($\beta = -0.81$; $p < 0.01$), tobacco use ($\beta = -0.51$; $p = 0.03$), and the presence of at least one APOE ε4 allele ($\beta = -0.81$; $p < 0.01$) were significantly associated with the composite measure of global cognitive function (NPZ-8). There were no significant associations of these variables with composite measures of memory (NPZ-3-mem) and psychomotor speed (NPZ-3-pm).

Discussion

This cross-sectional study used DTI to examine the micro-structural differences associated with cerebrovascular risk factors in HIV-infected subjects aged 50 years and older. Our findings suggest that subtle microstructural brain abnormalities are noted in the caudate and hippocampus in subjects with comorbid impairment in glucose metabolism.

In our study, only individuals with abnormal glucose metabolism but not other cerebrovascular risk factors were associated with microstructural differences in the caudate and hippocampus. More specifically, we found no differences by hypertension, dyslipidemia, smoking, or by APOE ε4 status. The differences demonstrated by impaired glucose metabolism were significant even when corrected for multiple comparisons. It is intriguing that differences were not found in other cerebrovascular risk factors which may be a result of the small sample size but also raises the possibility that the microstructural changes associated with abnormal glucose metabolism may not be mediated through atherosclerosis. For example, chronic hyperglycemia and hyperinsulinemia stimulate the formation of advanced glucosylated end-products, which can lead to overproduction of reactive oxygen species and resultant brain damage from oxidative stress (S Roriz-Filho et al. 2009). Alternatively, insulin-degrading enzyme (IDE) is the main clearance mechanism amyloid-beta (Aβ), and since IDE is more selective for insulin than Aβ, hyperinsulinemia may result in reduced neurotoxic Aβ clearance (S Roriz-Filho et al. 2009). Finally, hyperglycemia and hyperinsulinemia may also disrupt brain microstructure by inducing tau hyperphosphorylation (S Roriz-Filho et al. 2009). The increased diffusion (i.e., MD) and disorganization (i.e., FA) of water molecules in the caudate and hippocampus may be associated with increased edema from ischemia or inflammation associated with any of these possible mechanisms (Assaf and Pasternak 2008). Although past stimulant abuse has been associated with reduced microstructural integrity in the basal ganglia and hippocampus (Thames et al. 2011), there were no differences in frequency of past stimulant abuse between individuals with and without impaired glucose intolerance/diabetes in our study.

Abnormal glucose metabolism is highly prevalent in the HIV-infected population particularly as HIV-infected individuals live longer and prolonged exposure to cART increases the risk of hyperinsulinemia, impaired fasting glucose, impaired glucose tolerance, and ultimately diabetes mellitus (Brown et al. 2005; Justman et al. 2003; Tien et al. 2008).

Our DTI findings suggesting altered tissue integrity are supported by studies that have demonstrated insulin resistance and diabetes mellitus to be associated with cognitive dysfunction in HIV-infected individuals (Valcour et al. 2005, 2006, 2012).

Our study may have been underpowered to detect significant correlations between DTI parameters and other cerebrovascular risk factors, such as hypertension and hyperlipidemia. Furthermore, our study did not have a HIV-seronegative control group. Nevertheless, although our sample size was relatively small and we cannot exclude a spurious finding associated with post hoc analysis, significant differences were found in the caudate and hippocampus on DTI in our cohort of older HIV-infected subjects with abnormal glucose metabolism. This may illustrate the sensitivity of DTI to detect potential influences of abnormal glucose metabolism on brain microstructure. In summary, DTI can detect microstructural changes associated with abnormal glucose metabolism in the caudate and hippocampus of HIV-infected individuals, but further studies are warranted to determine if this finding reproducible.

Acknowledgments

BKN, KJK, DCC, and CMS are funded in part by research grants P20RR011091, U54NS43049, and U54RR026136. NJ and PT are funded in part by R01 EB008432 and EB 007813, and R01 AG040060 and a UCLA Medical Informatics Fellowship (NJ).

Glossary

Aβ	Amyloid-beta
APOE ε4	Apolipoprotein epsilon 4
ATP-III	Adult Treatment Panel III
BDI-II	Beck Depression Inventory II
cART	Combination antiretroviral therapy
DBP	Diastolic blood pressure
DTI	Diffusion tensor imaging
FA	Fractional anisotropy
FDR	False discovery rate
IDE	Insulin-degrading enzyme
MD	Mean diffusivity
NPZ-3-mem	Age- and education-adjusted composite score of memory
NPZ-3-pm	Age- and education-adjusted composite score of psychomotor speed
NPZ-8	Age- and education-adjusted composite score of global cognitive function
OGTT	2-h oral glucose tolerance test
PET	Positron emission tomography
ROIs	Regions of interest
SBP	Systolic blood pressure
SD	Standard deviation

References

American Diabetes Association. Standards of medical care in diabetes—2009. Diabetes Care. 2009; 32(Suppl 1):S13–S61. [PubMed: 19118286]

American Psychiatric Association. Diagnostic and statistical manual of mental disorders. 4th edn.. Washington, DC: American Psychiatric Association; 2000.

Assaf Y, Pasternak O. Diffusion tensor imaging (DTI)-based white matter mapping in brain research: a review. J Mol Neurosci. 2008; 34:51–61. [PubMed: 18157658]

Basser PJ, Mattiello J, LeBihan D. MR diffusion tensor spectroscopy and imaging. Biophys J. 1994a; 66:259–267. [PubMed: 8130344]

Basser PJ, Mattiello J, LeBihan D. Estimation of the effective self-diffusion tensor from the NMR spin echo. J Magn Reson. 1994b; 103:247–254.

Beck AT, Ward CH, Mendelson M, Mock J, Erbaugh J. An inventory for measuring depression. Arch Gen Psychiatry. 1961; 4:561–571. [PubMed: 13688369]

Becker JT, Kingsley L, Mullen J, et al. Vascular risk factors, HIV serostatus, and cognitive dysfunction in gay and bisexual men. Neurology. 2009; 73:1292–1299. [PubMed: 19841381]

Becker JT, Maruca V, Kingsley LA, et al. Factors affecting brain structure in men with HIV disease in the post-HAART era. Neuroradiology. 2011a; 54:113–121. [PubMed: 21424708]

Becker JT, Sanders J, Madsen SK, et al. Subcortical brain atrophy persists even in HAART-regulated HIV disease. Brain Imag Behav. 2011b; 5:77–85.

Benjamini Y, Hochberg Y. Controlling the false discovery rate: a practical and powerful approach to multiple testing. J R Biostatis Soc. 1995; 57:289–300.

Brown TT, Cole SR, Li X, et al. Antiretroviral therapy and the prevalence and incidence of diabetes mellitus in the multicenter AIDS cohort study. Arch Intern Med. 2005; 165:1179–1184. [PubMed: 15911733]

Brown TT, Xu X, John M, et al. Fat distribution and longitudinal anthropometric changes in HIV-infected men with and without clinical evidence of lipodystrophy and HIV-uninfected controls: a substudy of the Multicenter AIDS Cohort Study. AIDS Res Ther. 2009; 6:8. [PubMed: 19439092]

Chang L, Wong V, Nakama H, et al. Greater than age-related changes in brain diffusion of HIV patients after 1 year. J Neuroimmune Pharmacol. 2008; 3:265–274. [PubMed: 18709469]

Chen Y, An H, Zhu H, et al. White matter abnormalities revealed by diffusion tensor imaging in non-demented and demented HIV+ patients. NeuroImage. 2009; 47:1154–1162. [PubMed: 19376246]

Expert Panel on Detection, Evaluation, and Treatment of High Blood Cholesterol in Adults. Executive summary of The Third Report of The National Cholesterol Education Program (NCEP) Expert Panel on Detection, Evaluation, And Treatment of High Blood Cholesterol In Adults (Adult Treatment Panel III). JAMA. 2001; 285:2486–2497. [PubMed: 11368702]

Expert Panel on Detection, Evaluation, and Treatment of High Blood Cholesterol in Adults. Third Report of the National Cholesterol Education Program (NCEP) Expert Panel on Detection, Evaluation, and Treatment of High Blood Cholesterol in Adults (Adult Treatment Panel III) final report. Circulation. 2002; 106:3143–3421. [PubMed: 12485966]

Filippi CG, Ulug AM, Ryan E, Ferrando SJ, van Gorp W. Diffusion tensor imaging of patients with HIV and normal-appearing white matter on MR images of the brain. Ajnr. 2001; 22:277–283. [PubMed: 11156769]

Gongvatana A, Schweinsburg BC, Taylor MJ, et al. White matter tract injury and cognitive impairment in human immunodeficiency virus-infected individuals. J Neurovirol. 2009; 15:187–195. [PubMed: 19306228]

Gongvatana A, Cohen RA, Correia S, et al. Clinical contributors to cerebral white matter integrity in HIV-infected individuals. J Neurovirol. 2011; 17:477–486. [PubMed: 21965122]

Gorelick PB, Bowler JV. Advances in vascular cognitive impairment. Stroke; J Cereb Circ. 2010; 41:e93–e98.

Hoare J, Fouche JP, Spottiswoode B, et al. White-matter damage in clade C HIV-positive subjects: a diffusion tensor imaging study. J Neuropsychiatry Clin Neurosci. 2011; 23:308–315. [PubMed: 21948892]

Jellinger KA. Morphologic diagnosis of “vascular dementia”—a critical update. J Neurol Sci. 2008; 270:1–12. [PubMed: 18455191]

Justman JE, Benning L, Danoff A, et al. Protease inhibitor use and the incidence of diabetes mellitus in a large cohort of HIV-infected women. J Acquir Immune Defic Syndr. 2003; 32:298–302. [PubMed: 12626890]

Kallianpur KJ, Kirk GR, Sailasuta N, et al. Regional cortical thinning associated with detectable levels of HIV DNA. Cereb Cortex. 2011

Kuper M, Rabe K, Esser S, et al. Structural gray and white matter changes in patients with HIV. J Neurol. 2011; 258:1066–1075. [PubMed: 21207051]

Lamport DJ, Lawton CL, Mansfield MW, Dye L. Impairments in glucose tolerance can have a negative impact on cognitive function: a systematic research review. Neurosci Biobehav Rev. 2009; 33:394–413. [PubMed: 19026680]

Leow A, Huang SC, Geng A, et al. Inverse consistent mapping in 3D deformable image registration: its construction and statistical properties. Inf Process Med Imaging. 2005; 19:493–503. [PubMed: 17354720]

McMurtray, A.; Kwee, S.; Grace, T.; Shikuma, C. Changes in cerebral glucose metabolism associated with the presence of the apolipoprotein E4 allele in older HIV seropositive individuals. 11th RCMI International Symposium on Health Disparities; Honolulu, Hawaii. 2008.

Nakamoto, BK.; Jahanshad, N.; Kallianpur, K.; Shikuma, C.; Valcour, VG.; Thompson, PM. CROI. San Francisco, CA: 2010 Feb 16–19. Impact of ApoE and cerebrovascular risk factors on brain structure and cognition in HIV in the HAART era.

Nakamoto BK, Valcour VG, Kallianpur K, et al. Impact of cerebrovascular disease on cognitive function in HIV-infected patients. J Acquir Immune Defic Syndr. 2011; 57:e66–e68. [PubMed: 21860354]

Navia BA, Cho ES, Petito CK, Price RW. The AIDS dementia complex: II. Neuropathology. Ann Neurol. 1986; 19:525–535. [PubMed: 3014994]

Ovbiagele B, Nath A. Increasing incidence of ischemic stroke in patients with HIV infection. Neurology. 2011; 76:444–450. [PubMed: 21248273]

Pfefferbaum A, Rosenbloom MJ, Adalsteinsson E, Sullivan EV. Diffusion tensor imaging with quantitative fibre tracking in HIV infection and alcoholism comorbidity: synergistic white matter damage. Brain. 2007; 130:48–64. [PubMed: 16959813]

Pfefferbaum A, Rosenbloom MJ, Rohlfing T, Kemper CA, Deresinski S, Sullivan EV. Frontostriatal fiber bundle compromise in HIV infection without dementia. AIDS (London, England). 2009; 23:1977–1985.

Ragin AB, Wu Y, Storey P, Cohen BA, Edelman RR, Epstein LG. Diffusion tensor imaging of subcortical brain injury in patients infected with human immunodeficiency virus. J Neurovirol. 2005; 11:292–298. [PubMed: 16036809]

S Roriz-Filho J, Sa-Roriz TM, Rosset I, et al. (Pre)diabetes, brain aging, and cognition. Biochim Biophys Acta. 2009; 1792:432–443. [PubMed: 19135149]

Schmitt FA, Bigley JW, McKinnis R, Logue PE, Evans RW, Drucker JL. Neuropsychological outcome of zidovudine (AZT) treatment of patients with AIDS and AIDS-related complex. N Engl J Med. 1988; 319:1573–1578. [PubMed: 3059187]

Shiramizu B, Paul R, Williams A, et al. HIV proviral DNA associated with decreased neuropsychological function. J Neuropsychiatry Clin Neurosci. 2007; 19:157–163. [PubMed: 17431062]

Strauss, E.; Sherman, EMS.; Spreen, O. A compendium of neuropsychological tests: administration, norms, and commentary. 3rd edn.. New York: Oxford University Press; 2006.

Thames AD, Foley JM, Panos SE, et al. Past stimulant abuse is associated with reduced basal ganglia and hippocampal integrity in older HIV+ adults. A Diffusion Tensor Imaging Study. 2011; 2:129–134.

Tien PC, Schneider MF, Cole SR, et al. Antiretroviral therapy exposure and insulin resistance in the Women's Interagency HIV study. J Acquir Immune Defic Syndr. 2008; 49:369–376. [PubMed: 19186350]

U.S. Preventive Services Task Force. Screening for high blood pressure: U.S. Preventive Services Task Force reaffirmation recommendation statement. Ann Intern Med. 2007; 147:783–786. [PubMed: 18056662]

Valcour VG, Shikuma CM, Shiramizu BT, et al. Diabetes, insulin resistance, and dementia among HIV-1-infected patients. J Acquir Immune Defic Syndr. 2005; 38:31–36. [PubMed: 15608521]

Valcour VG, Sacktor NC, Paul RH, et al. Insulin resistance is associated with cognition among HIV-1-infected patients: the Hawaii Aging With HIV cohort. J Acquir Immune Defic Syndr. 2006; 43:405–410. [PubMed: 17099311]

Valcour V, Maki P, Bacchetti P, et al. Insulin resistance and cognition among HIV-infected and HIV-uninfected adult women: The Women's Interagency HIV Study. AIDS Res Hum Retroviruses. 2012; 28(5):447–453. [PubMed: 21878059]

Wright EJ, Grund B, Robertson K, et al. Cardiovascular risk factors associated with lower baseline cognitive performance in HIV-positive persons. Neurology. 2010; 75:864–873. [PubMed: 20702792]

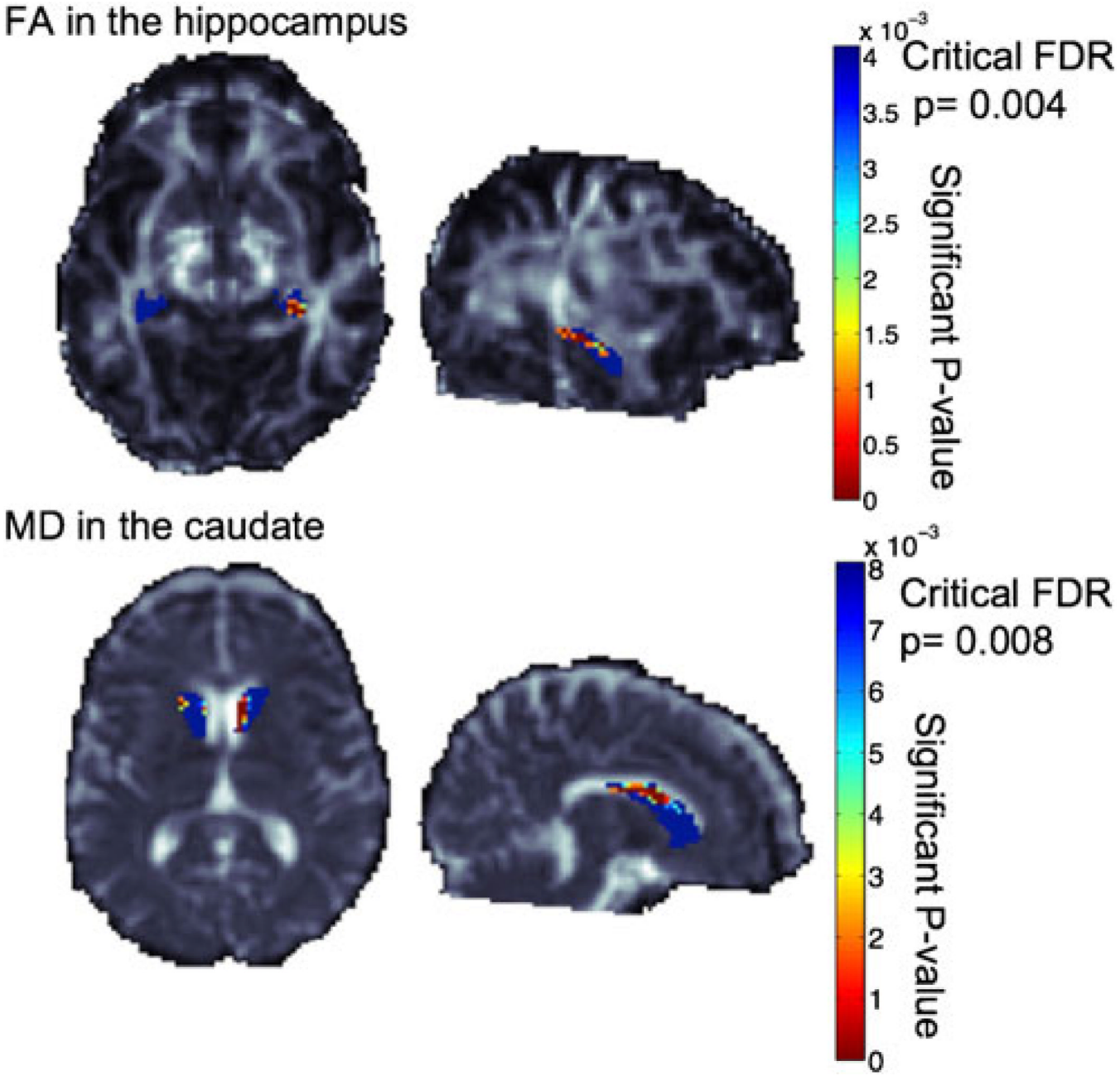

Fig. 1.

Top panel shows the hippocampal segmentation over the FA image. Voxelwise associations of FA within the hippocampus revealed a significant association with impaired glucose intolerance/diabetes mellitus. *Bottom panel* shows the caudate segmentation over the MD image. Voxelwise associations of MD within the caudate revealed a significant association with impaired glucose intolerance/diabetes mellitus. More significant voxels are colored *reddish yellow*. Voxels that did not pass the false discovery rate (*FDR*) correction for multiple tests are colored *blue*. The FDR critical *p* values are 0.004 and 0.008, respectively. Note that the higher the FDR critical *p* values (i.e., the closer to 0.05), the greater the association. Images are shown in radiological convention, and the sagittal images are of the left hemisphere. *FA* fractional anisotropy, *FDR* false discovery rate, *MD* mean diffusivity

Table 1

Demographic and clinical characteristics of subjects

	N=22
Mean age, years (SD; range)	58 (6; 50 73)
% male	86 (19/22)
% non-Hispanic white	77 (17/22)
% Hispanic white	5 (1/22)
% Asian	9 (2/22)
% Native American	5 (1/22)
% Native Hawaiian	5 (1/22)
Mean years of education (SD; range)	16 (2; 12–20)
HIV-associated parameters	
Mean years HIV-positive (SD; range)	17 (2–26)
% on HAART	95 (21/22)
% on protease inhibitor	18 (4/22)
% with current CD4+ count >200 cells/μL	100 (22/22)
% with undetectable HIV RNA viral load (<50 copies/mL)	82 (18/22)
Mean self-reported lowest ever CD4 count, cells/μL (SD; range)	210 (171; 1–450)
% with history of prior stimulant use	64 (14/22)
Cerebrovascular risk factors	
Mean body mass index, kg/m (Wright et al. 2010) (SD)	24 (3)
% with abdominal obesity[a]	0 (0/22)
Mean waist circumference, cm (SD, range)	91 (7; 76–102)
% with impaired glucose tolerance	41 (9/22)
% with adult-onset diabetes mellitus	18 (4/22)
% with hypertension	45 (10/22)50
Mean SBP, mmHg (SD, range)	126 (18; 99–159)
Mean DBP, mmHg (SD, range)	74 (10; 52–89)
% with fasting LDL≥100 mg/dL	50 (11/22)
Mean fasting LDL, mg/dL (SD, range)	112 (44; 52–226)
% with fasting triglycerides ≥ 150 mg/dL	36 (8/22)
Mean fasting triglycerides, mg/dL (SD, range)	169 (128; 36–341)
% with fasting HDL cholesterol <40 mg/dL in men or <50 mg/dL in women	64 (14/22)
Mean fasting HDL cholesterol, mg/dL (SD; range)	40 (19; 18–110)
% with metabolic syndrome	32 (7/22)
% with past or present smoking history	45 (10/22)
Mean pack years (SD, range)	19 (11; 1–30)
% with at least one APOE e4 allele	40 (9/22)
% with white matter hyperintensities on MRI	36 (8/22)
Mean Beck Depression Inventory score (SD, range)	7 (4, 1–15)

APOE ε4 allele apolipoprotein epsilon 4 allele, *DBP* diastolic blood pressure, *HAART* highly active antiretroviral therapy, *MI* myocardial infarction, *SBP* systolic blood pressure, *SD* standard deviation

[a]Abdominal obesity was defined as a waist circumference in men greater than 102 cm (40 in.) and in women greater than 88 cm (35 in.) (Detection et al. 2001)

Table 2

Association of vascular risk factors and DTI parameters

	Abnormal glucose metabolism[a]			**Hypertension**			**Dyslipidemia**		
	Present	**Absent**	**FDR critical *p* value**	**Present**	**Absent**	**FDR critical *p* value**	**Present**	**Absent**	**FDR critical *p* value**
Caudate MD	1.33 (0.65)	1.14 (0.54)	0.008	1.32 (0.63)	1.19 (0.58)	NS	1.31 (0.63)	1.20 (0.58)	NS
Caudate FA	0.19 (0.10)	0.21 (0.11)	0.002	0.20 (0.10)	0.21 (0.11)	NS	0.19 (0.10)	0.21 (0.12)	NS
Hippocampus MD	1.16 (0.27)	1.01 (0.20)	NS	1.15 (0.27)	1.05 (0.23)	NS	1.15 (0.26)	1.05 (0.23)	NS
Hippocampus FA	0.16 (0.08)	0.19 (0.09)	0.004	0.17 (0.08)	0.18 (0.09)	NS	0.17 (0.08)	0.18 (0.09)	NS
Thalamus MD	1.01 (0.47)	0.92 (0.36)	NS	1.02 (0.51)	0.93 (0.35)	NS	1.02 (0.47)	0.93 (0.39)	NS
Thalamus FA	0.29 (0.10)	0.29 (0.09)	NS	0.30 (0.10)	0.29 (0.09)	NS	0.28 (0.09)	0.30 (0.09)	NS
Putamen MD	0.75 (0.7)	0.75 (0.06)	NS	0.76 (0.06)	0.74 (0.07)	NS	0.76 (0.06)	0.74 (0.07)	NS
Putamen FA	0.25 (0.07)	0.22 (0.07)	NS	0.24 (0.07)	0.25 (0.07)	NS	0.24 (0.08)	0.24 (0.06)	NS
Globus pallidus MD	0.70 (0.14)	0.65 (0.15)	NS	0.69 (0.14)	0.66 (0.15)	NS	0.70 (0.14)	0.65 (0.15)	NS
Globus pallidus FA	0.37 (0.09)	0.41 (0.09)	NS	0.38 (0.08)	0.39 (0.09)	NS	0.37 (0.09)	0.40 (0.08)	NS
Corpus callosum MD	0.90 (0.17)	0.90 (0.03)	NS	1.02 (0.19)	0.91 (0.03)	NS	1.01 (0.19)	0.91 (0.03)	NS
Corpus callosum FA	0.42 (0.05)	0.44 (0.03)	NS	0.41 (0.05)	0.45 (0.02)	NS	0.43 (0.05)	0.44 (0.02)	NS
Frontal lobe WM MD	1.09 (0.32)	1.02 (0.29)	NS	1.10 (0.32)	1.01 (0.29)	NS	1.10 (0.33)	1.02 (0.28)	NS
Frontal lobe WM FA	0.20 (0.11)	0.20 (0.12)	NS	0.20 (0.11)	0.20 (0.12)	NS	0.20 (0.11)	0.20 (0.12)	NS
Parietal lobe WM MD	1.02 (0.36)	0.96 (0.33)	NS	1.02 (0.37)	0.96 (0.33)	NS	1.02 (0.36)	0.97 (0.33)	NS
Parietal lobe WM FA	0.20 (0.13)	0.21 (0.13)	NS	0.20 (0.12)	0.21 (0.13)	NS	0.20 (0.13)	0.21 (0.13)	NS
Temporal lobe WM MD	1.00 (0.35)	0.92 (0.31)	NS	1.00 (0.36)	0.93 (0.31)	NS	1.00 (0.35)	0.93 (0.32)	NS
Temporal lobe WM FA	0.18 (0.08)	0.19 (0.09)	NS	0.18 (0.08)	0.19 (0.09)	NS	0.18 (0.09)	0.19 (0.09)	NS
Occipital lobe WM MD	0.96 (0.26)	0.89 (0.23)	NS	0.95 (0.27)	0.91 (0.23)	NS	0.95 (0.26)	0.91 (0.24)	NS
Occipital lobe WM FA	0.17 (0.08)	0.18 (0.09)	NS	0.17 (0.08)	0.17 (0.09)	NS	0.17 (0.08)	0.17 (0.09)	NS
	Past or current tobacco use			Metabolic syndrome			At least one APOE e4 allele present		
	Present	Absent	FDR critical *p* value	Present	Absent	FDR critical *p* value	Present	Absent	FDR critical *p* value
Caudate MD	1.25 (0.59)	1.26 (0.61)	NS	1.33 (0.65)	1.22 (0.58)	NS	1.25 (0.60)	1.26 (0.60)	NS
Caudate FA	0.20 (0.11)	0.20 (0.10)	NS	0.20 (0.10)	0.20 (0.11)	NS	0.21 (0.11)	0.19 (0.10)	NS
Hippocampus MD	1.10 (0.24)	1.10 (0.24)	NS	1.16 (0.28)	1.07 (0.23)	NS	1.11 (0.26)	1.09 (0.24)	NS
Hippocampus FA	0.18 (0.08)	0.17 (0.08)	NS	0.16 (0.08)	0.18 (0.08)	NS	0.17 (0.08)	0.17 (0.08)	NS
Thalamus MD	0.98 (0.43)	0.97 (0.42)	NS	0.99 (0.46)	0.97 (0.41)	NS	0.98 (0.45)	0.97 (0.41)	NS
Thalamus FA	0.29 (0.09)	0.30 (0.09)	NS	0.30 (0.10)	0.29 (0.09)	NS	0.30 (0.10)	0.29 (0.09)	NS

J Neurovirol. Author manuscript; available in PMC 2013 August 01.

	Abnormal glucose metabolism[a]			Hypertension			Dyslipidemia		
	Present	**Absent**	**FDR critical *p* value**	**Present**	**Absent**	**FDR critical *p* value**	**Present**	**Absent**	**FDR critical *p* value**
Putamen MD	0.76 (0.06)	0.74 (0.06)	NS	0.75 (0.08)	0.75 (0.06)	NS	0.76 (0.06)	0.74 (0.06)	NS
Putamen FA	0.23 (0.07)	0.25 (0.07)	NS	0.26 (0.07)	0.23 (0.07)	NS	0.23 (0.07)	0.25 (0.07)	NS
Globus pallidus MD	0.67 (0.16)	0.69 (0.13)	NS	0.69 (0.15)	0.67 (0.14)	NS	0.70 (0.13)	0.66 (0.15)	NS
Globus pallidus FA	0.39 (0.10)	0.38 (0.08)	NS	0.39 (0.08)	0.39 (0.09)	NS	0.37 (0.08)	0.40 (0.09)	NS
Corpus callosum MD	0.96 (0.14)	0.96 (0.15)	NS	0.99 (0.19)	0.94 (0.12)	NS	0.96 (0.15)	0.96 (0.14)	NS
Corpus callosum FA	0.43 (0.05)	0.43 (0.03)	NS	0.43 (0.04)	0.43 (0.04)	NS	0.42 (0.05)	0.44 (0.04)	NS
Frontal lobe WM MD	1.05 (0.30)	1.07 (0.32)	NS	1.08 (0.33)	1.05 (0.29)	NS	1.07 (0.32)	1.05 (0.30)	NS
Frontal lobe WM FA	0.20 (0.12)	0.20 (0.11)	NS	0.20 (0.12)	0.20 (0.11)	NS	0.20 (0.11)	0.20 (0.12)	NS
Parietal lobe WM MD	0.98 (0.34)	1.00 (0.35)	NS	1.01 (0.37)	0.99 (0.34)	NS	1.00 (0.36)	0.99 (0.34)	NS
Parietal lobe WM FA	0.20 (0.13)	0.21 (0.13)	NS	0.20 (0.13)	0.20 (0.13)	NS	0.20 (0.13)	0.20 (0.13)	NS
Temporal lobe WM MD	0.96 (0.33)	0.97 (0.34)	NS	1.00 (0.37)	0.95 (0.32)	NS	0.97 (0.34)	0.96 (0.33)	NS
Temporal lobe WM FA	0.19 (0.09)	0.19 (0.09)	NS	0.18 (0.09)	0.19 (0.09)	NS	0.19 (0.09)	0.18 (0.09)	NS
Occipital lobe WM MD	0.92 (0.25)	0.94 (0.25)	NS	0.96 (0.27)	0.92 (0.24)	NS	0.93 (0.26)	0.93 (0.24)	NS
Occipital lobe WM FA	0.17 (0.08)	0.17 (0.08)	NS	0.17 (0.08)	0.17 (0.08)	NS	0.17 (0.08)	0.17 (0.08)	NS

MD values are expressed as 10^{-3}

[a]Abnormal glucose metabolism is defined as impaired fasting glucose, impaired glucose intolerance, or diabetes mellitus